MEASUREMENT OF THE CHARGED SPLASH AND RE-ENTRANT ALBEDO OF THE COSMIC RADIATION*+

Satya Dev Verma**
Enrico Fermi Institute for Nuclear Studies and
Department of Physics
University of Chicago
Chicago, Illinois 60637

Laboratory for Astrophysics and Space Research

Preprint No. EFINS 66-71

July 1966

* This work was supported in part by the National Aeronautics and Space Administration under grant NASA NsG 144-61.

+ A thesis submitted to the Department of Physics, The University of Chicago, Chicago, Illinois, in partial fulfillment of the requirements of the Ph.D. degree..

** On leave from Tata Institute of Fundamental Research, Bombay-5, India.

MEASUREMENT OF THE CHARGED SPLASH AND RE-ENTRANT ALBEDO OF THE COSMIC RADIATION*+

Satya Dev Verma**
Enrico Fermi Institute for Nuclear Studies and
Department of Physics
University of Chicago
Chicago, Illinois 60637

Abstract

12219

A study of the flux and energy spectrum of the proton and electron components of the splash and re-entrant cosmic ray albedo has been made in mid-1965 at balloon altitude over Palestine, Texas (geomagnetic cut-off 4.9 BV). The energy spectrum and the flux of the splash and the re-entrant albedo protons has been measured in the energy range from 37 MeV to 334 MeV, at an atmospheric depth of about 4 g/cm^2. The two spectra agree within experimental errors and can be represented by the power laws

$$\left(\frac{dJ}{dE}\right)_{Sp.Pr.} = (6 \pm 4)\left(\frac{E}{10}\right)^{-(1.4 \pm .2)} \quad (m^2 \text{ sec ster MeV})^{-1}, \quad 37 \leq E \leq 334 \text{ MeV}$$

$$\left(\frac{dJ}{dE}\right)_{Re.Pr.} = (13 \pm 9)\left(\frac{E}{10}\right)^{-(1.7 \pm .3)} \quad (m^2 \text{ sec ster MeV})^{-1}, \quad 75 \leq E \leq 350 \text{ MeV}$$

Ray calculated the flux of the re-entrant albedo protons at 85 MeV, and obtained .41

over

* This work was supported in part by the National Aeronautics and Space Administration under grant NASA NsG 144-61.

+ A thesis submitted to the Department of Physics, The University of Chicago, Chicago, Illinois, in partial fulfillment of the requirements of the Ph.D. degree.

** On leave from Tata Institute of Fundamental Research, Bombay-5, India.

$(m^2 \text{ sec ster. MeV})^{-1}$ for a geomagnetic cut-off energy of 1 BeV. His calculation is in agreement with the present measurements.

The energy spectrum and the flux of the splash and the re-entrant albedo electrons has been measured in an energy range from 10 MeV to 1100 MeV, also at a depth of about 4 g/cm^2. The splash and re-entrant albedo electron energy spectra at the top of the atmosphere are well represented by power law spectra

$$\left(\frac{dJ}{dE}\right)_{Sp.El.} = (5.4 \pm 0.5)\, 10^2\, E^{-(1.29 \pm .06)} \qquad (m^2 \text{sec ster MeV})^{-1}, \quad 10 \leq E \leq 1100 \text{ MeV}$$

$$\left(\frac{dJ}{dE}\right)_{Re.El.} = (5.9 \pm 0.9)\, 10^2\, E^{-(1.44 \pm .09)} \qquad (m^2 \text{sec ster MeV})^{-1}, \quad 20 \leq E \leq 1250 \text{ MeV}$$

where J is the electron flux and E is the kinetic energy. The two spectra agree within experimental errors.

AUTHOR

I. Introduction

Primary cosmic ray particles impinging on the atmosphere interact with air nuclei and produce secondary particles. Some of these secondary particles move in the upward direction, and have been named "splash albedo." Some of the charged splash albedo particles after leaving the atmosphere may be trapped in bound orbits, in which case they will eventually return to the earth. These are called "re-entrant albedo." Treiman [1953] was the first to point out that the re-entrant albedo particles return very closely to the same geomagnetic latitude from which they left the earth in the opposite hemisphere, although the longitude is generally changed. They will have energies below the geomagnetic cut-off energy. Thus, disregarding atmospheric secondaries, one would expect the downward moving particles below the vertical geomagnetic cut-off energy to be re-entrant albedo, and those above the cut-off energy to be primary particles. In order to clearly observe the re-entrant albedo energy spectrum and flux, an experiment should be carried out well below the cut-off energy. There are few calculations and measurements of the spectrum of the charged albedo particles. We therefore, carried out 3 balloon flights to measure the proton and electron energy spectra at Palestine, Texas for rigidities well below the geomagnetic cut-off (4.9 BV) at this location. In this experiment we successfully discriminated electrons and protons and independently measured the splash and re-entrant proton albedo fluxes and energy spectra in the 37 to 334 MeV energy range and electron albedo fluxes and energy spectra in the 10 to 1100 MeV energy interval. In earlier experiments no clear distinction between electrons and protons could be made and in most cases only flux values over broad energy intervals rather than detailed energy spectra were obtained. Hasegawa et al [1965] have measured the proton splash albedo flux

at Sioux Falls, S. D. (cut-off 1.7 BV) in the 66 MeV to 300 MeV energy range. Near the equator, this flux was measured by McDonald [1958] at Guam, Marianas Islands in the 270 MeV to 750 MeV energy interval. At geomagnetic latitudes 53°N and 55°N, McDonald and Webber [1959] estimated the sum of the flux of both splash and re-entrant proton albedo in the 100 to 350 MeV energy region without being able to distinguish between the two. Ormes and Webber [1964] have estimated the intensity of the splash and re-entrant albedo protons at 7.4 g/cm^2 at Minneapolis, Minnesota.

In the case of the re-entrant electron albedo, Bleeker et al. [1965] have measured the differential energy spectrum in the 200 to 1400 MeV energy range at 10 g/cm^2 in a balloon flight from DeBilt, Netherlands (cut-off 1.9 BV). The flux of the re-entrant electrons was also measured by Schmoker and Earl [1965] at Minneapolis, Minnesota (cut-off 1.4 BV) in the 45 MeV to 150 MeV energy range and at San Angelo, Texas (cut-off 4.6 BV) in the energy interval from 1 BeV to 4.5 BeV. Daniel and Stephens [1965] have measured the flux below 7 BeV at Hyderabad, India (cut-off 17 BV). In section VI we shall compare these earlier results with our own measurements.

The experiments requires the identification and measurement of the energy of electrons and protons in the 10 to 1000 MeV energy region. Suitable parameters for this measurement are the particle energy loss $(\frac{dE}{dx})$ and its residual range (R). The instrument which we used was capable of measuring these parameters simultaneously. In addition, stopping electrons and protons were distinguished by the use of a Cerenkov counter. The apparatus is discussed in detail in section II.

II. Apparatus

The apparatus used in this experiment is a modification of an instrument which was previously designed and used by Vogt [1962] and Meyer and Vogt [1963]. In Fig. 1 we present a cross-section view of the detector system. T is a plastic scintillation counter and I is a NaI (Tl) scintillation counter. A vertically incident charged particle which triggers T and I constitutes an event. The particle energy loss ($\frac{dE}{dX}$) is measured in counter I and is analyzed by a 64-channel pulse height analyzer. Six plastic scintillation counters R_1 to R_6 are embedded in a lead absorber. These counters determine the range of those charged particles which stop in the lead absorber. For electrons they determine the penetration depth of an electron photon cascade. The geometric factor of the telescope is 1.91 cm^2 ster.

In order to discriminate better between electrons and protons and to measure independently the energy spectra of both kinds of particles, the original instrument used by Vogt [1962] was modified in several ways.

(1) A lucite Cerenkov counter C_1 was used in place of the second range counter and additional range counter (R_6) was added below the lead absorber. Electrons and protons stopping between C_1 and R_6 can be distinguished from each other by the counter C_1, since only the stopping electrons can produce a pulse in C_1 but not the stopping protons. However, those μ-mesons and π-mesons which happen to stop between R_3 and R_6 can not be distinguished from electrons since they also may produce a pulse in C_1. Their flux is small and will be corrected for in the later discussion. The electrons and protons which stop between counter I and counter C_1 can be distinguished by their energy loss in counter I. Protons with energy in excess of 900 MeV not only penetrate the entire lead absorber but also produce a pulse in C_1.

Therefore, these protons can not be distinguished from electron showers which penetrate the absorber.

(2) A second lucite Cerenkov counter 'C_2' was added below the R_6 counter. This Cerenkov counter was painted dull black on its top surface and sides. It therefore responds to charged particles moving in the direction from T to C_2 with speed greater than the Cerenkov threshold for C_2 but is not triggered by particles moving in the opposite direction. The directional performance of C_2 was checked at sea level using cosmic ray muons. The rejection ratio of this counter is about 50:1 for penetrating particles. It should be kept in mind that for stopping particles there is no ambiguity of the direction of motion.

(3) We also added a plastic scintillation guard counter A_5 to a set of four guard counters A_1 to A_4 which are placed around the lead-counter assembly.

The apparatus in its present form is suitable for measurement of the electrom spectrum between 10 MeV and about 1100 MeV and of the proton spectrum in the energy range from 28 MeV to 334 MeV separately. High energy electrons ($\gtrsim$ 1100 MeV) and protons ($E \geq 900$ MeV) all fall into one group, but their direction of motion (up or down) can be recorded.

III. Balloon Flights

Two balloon flights were launced from Palestine, Texas (cut-off 4.9 BV) on May 20-21 and Sept. 25, 1965. The floating depth of the balloon in each case was about 4.0 g/cm^2. The apparatus was oriented towards the zenith to observe the fluxes and energy spectra of the re-entrant albedo particles. The results reported here are based on data collected during eight hours from these flights. The launch site at Palestine was selected to keep the energy range which we wished to study

well below the vertical geomagnetic cut-off energy, so that no charged primary cosmic ray particles would be present in this energy interval.

One further balloon flight was carried out from the same launch site on May 29-30, 1965. In this flight the apparatus was inverted and oriented vertically towards the earth to observe the fluxes and energy spectra of the splash albedo particles. The results for the splash albedo protons and electrons are based upon eight hours of measurements. The apparatus floated at 3.8 g/cm^2 of residual atmosphere.

IV. Data Analysis

The data were recorded on magnetic tape aboard the flight gondola as well as telemetered to the ground and recorded on teletype paper tape. At a later time, the magnetic tape data and the telemetered data were compared to reject possible noise events. The proton energy spectra were obtained from their energy loss ($\frac{dE}{dX}$) and their residual range (R), using the range-energy relations given by Rich and Madey [1954]. In the case of the electrons, we were able to make use of a calibration run with a beam of mono-energetic electrons at several energies (100, 300, 500, 700, and 900 MeV), carried out by R. Vogt*. The similarity of the

---

* We are grateful to Professor R. Vogt for making available to us his calibration data and to the California Institute of Technology Synchrotron group for the use of their facilities.

apparatus permitted the direct use of this calibration. The equipment was also calibrated before flights using relativistic muons in vertically up and inverted positions. The energy loss of the relativistic protons provided an inflight calibration of the detector and pulse height analyzer.

V. (A) Corrections Applied to the Proton Flux

(1) Nuclear Interactions in the Lead Absorber

Protons in the energy range from 37 to 334 MeV are identified by a simultaneous measurement of the energy-loss, the residual range and absence of an output from the Cerenkov counter C_1. Their range was converted into energy by using the range-energy relation and assuming ionization losses only. However, a fraction of the protons will make nuclear interactions in the lead absorber. To correct for the protons which have interacted in the lead, two possibilities must be considered:

a. Secondaries produced in the interaction trigger at least one of the five anticoincidence counters (A_1 to A_5). Such an event is recorded with the guard counter on, we call it an "AC ON" event.

b. If none of the secondaries produced in the interaction triggers any of the guard counters, then this event will be analyzed as an "AC OFF" event. However, in this case the range will normally not be related to the energy loss in the same way it would if an interaction had not taken place. In such cases, the residual range is determined by the most penetrating charged secondary. A correction is to be applied for both types of events. Vogt [1962] has calculated this correction for protons having energy between 37 MeV to 334 MeV

for the detector system which we used. The correction is about 5% in the lowest energy interval and increases as the energy of protons increases, up to about 35% in the highest energy interval. We modified his corrections for the changes which were made in the assembly and applied them to the proton data.

We have considered the effect of multiple scattering of protons in the lead absorber. This scattering leads to the loss of a fraction of the protons leaving the absorber on the sides. The effect is largest for the larger ranges. However, a calculation shows that the correction amounts to 3% for protons which reach the full depth of the absorber and is correspondingly smaller for shorter ranges. Since other errors are appreciably larger, we have not included a correction for this effect in our final data.

(2) Secondary Protons Produced in the Atmosphere

The contributions of secondary protons in various range intervals and for various depths over Fort Churchill were also computed by Vogt [1962], using the production rate of stars of different prong numbers as a function of atmospheric depth as given by Lord [1951]. Lord obtained data for two locations, $\lambda = 28^{\circ}N$ and $\lambda = 54^{\circ}N$. We interpolated his data to obtain the star production rate for Palestine, Texas $\lambda = 41^{\circ}N$. This rate of star production differs by the factor 3.3 ± 0.6 from the rate for Fort Churchill used by Vogt [1962]. Thus, using this constant factor and the flux of secondary protons calculated by Vogt for Fort Churchill, we calculated the flux of the secondary protons in different range (or energy) intervals and for various atmospheric depths over Palestine, Texas. Some uncertainty is involved in these calculations due to the change of the star production rate with the

solar cycle. This uncertainty is small, about 3% as compared with the error in the interpolated rates of star production, which is about 20%. The flux of secondary protons in various range intervals at 4.4 g/cm^2 is given in the fourth column of Table 1. The 4.4 g/cm^2 correspond to an atmosphere depth of 4.0 g/cm^2, the remaining 0.4 g/cm^2 being due to local matter in the gondola above the telescope, in equivalent thickness of air.

It is desirable to compare the calculated flux of secondary protons at various depths with the measured altitude dependence of the proton flux. This can be done in the following way. The proton energy spectrum as measured at floating altitude (4 g/cm^2) was corrected for secondary protons (see Table 1, columns 3 and 4) and extrapolated to the top of the atmosphere by considering the ionization loss of the protons (columns 5 and 6, Table 1). Using this spectrum and the ionization loss, an absorption curve for the incident re-entrant protons was calculated. This is shown as a dashed-dot line in Figure 2. The flux of the calculated secondary protons, shown as a solid line to a depth of 10 g/cm^2 and linearly extrapolated to 30 g/cm^2 (dotted line) was then added to the flux of the incident protons at each depth up to 30 g/cm^2. The resulting curve (shown as a dashed line) can be compared with the measured proton flux as a function of atmospheric depth. The shape of the calculated altitude curve fits the experimental data well to about 30 g/cm^2. It should be noted that the altitude curve for the secondaries has not been adjusted or normalized to the experimental points.

B. Calibration and Corrections Applied to the Electron Flux

(1) Calibration:

Electrons are identified by a simultaneous measurement of the energy-loss, penetration of the electron-photon cascade (Range) and Cerenkov light emission in the counter C_1. Since the electrons produce an electron-photon cascade whose

range is not well defined, there exists the problem of converting the observed "range" of electrons into an energy. To solve this problem, the apparatus was calibrated with 100, 300, 500, 700, and 900 MeV electron beams and the range distribution was measured for each energy. There are two additional problems to be considered. First, in a fraction of the cases an electron shower penetrates the lead absorber and electrons emerge from the side of the absorber and trigger one or more guard counters. Secondly, due to the presence of gamma rays alone in a part of the cascade shower, one or two range counters may not be triggered in sequence. With the help of the calibration runs we obtained (i) the fraction of cases in which an electron shower triggers the guard counters, and (ii) the fraction of events where a range counter was missed at various energies. With this information, it is possible to convert the range spectrum of electrons into an energy spectrum.

(2) Secondary Electrons and Muons Produced in the Atmosphere

Among the downward moving electrons in the energy region under consideration, there is a considerable amount of secondary electrons and a small amount of secondary muons present. The flux and spectrum of secondary electrons in the top layers of the earth's atmosphere have been calculated by Verma [1966] for various depths and different places including Palestine, Texas. The calculated secondary spectrum at a depth of 4 g/cm^2 for Palestine, Texas is given in Figure 8. This spectrum was used to estimate the secondary electron contributions. In Figure 3, we compared the calculated flux of secondary electrons as a function of depth with the measured altitude dependence of the electron flux (in two energy intervals, 10 to 100 MeV and 100 to 1100 MeV). The procedure adopted is the same as that described for the case of protons in Sec. V(A) (2). The calculated secondary flux

is plotted as a solid line up to 10 g cm^{-2} and linearly extrapolated to 30 g cm^{-2}. The absorption curve for re-entrant electrons is plotted as a dashed-dot line. It includes energy loss by ionization and by bremsstrahlung. Adding the two curves we obtained the dashed line which may be compared with the measured electron flux as a function of depth. The agreement is good to about 30 g/cm^2.

Stopping muons in the energy range 60 - 160 MeV cannot be distinguished from absorbed electron showers (300 to 1100 MeV) in our apparatus. In order to correct for the vertically downward moving muons, a calculation was made which showed that the flux of stopping muons is about 5% or less of the flux of the stopping electrons. In view of the fact that the experimental errors are much larger than the correction for stopping muons, we left the data uncorrected.

(C) Dead Time Correction:

The data recording system uses one second out of each minute to record temperature, pressure and two counting rates. Also a dead time (.1 sec) is needed to record and process each individual event. Thus the fraction of time lost is given by $\frac{\Delta T}{T} = \frac{1 + N\tau}{60}$ where N are counts per minute and τ is the dead time in seconds. We applied the lost time correction to all data.

VI. Results and Discussion: (A) Proton Albedo

(1) Proton Splash Albedo Flux vs. Depth.

The flux of splash albedo protons was observed at a floating altitude of 3.8 g/cm^2, with the apparatus oriented vertically toward the earth. This flux consists of particles produced in a large thickness of the atmosphere below the apparatus and should therefore not vary in the uppermost layers of the atmosphere. In Figure 4 the splash albedo flux is plotted vs. atmospheric depth in g/cm^2. The change of the flux between 60 and 3.8 g/cm^2 is less than the error of each point. Therefore,

within the errors, an extrapolation to the top of the atmosphere yields the same flux as observed at float altitude.

(2) Comparison Between Splash and Re-entrant Proton Albedo Energy Spectra

The energy spectrum of the proton splash albedo in the 37 to 334 MeV energy interval was observed at a depth of 3.8 g/cm^2. We have shown this spectrum in Figure 5, after correcting for nuclear interactions of protons in the lead absorber and for the dead time. In the same figure we have also plotted for comparison the measurements obtained by other investigators. Hasegawa et al [1965] have measured the flux of splash protons in the 66 MeV to 300 MeV energy range at Sioux Falls, S. D. (geomagnetic cut-off 1.7 BV). The flux between 270 and 700 MeV has been measured at Guam (cut-off 17 BV) by McDonald [1958]. At geomagnetic latitude 53°N and 55°N, using the altitude dependence of the flux of protons below the Cerenkov threshold ($100 \leq E \leq 350$ MeV) and subtracting the contribution of the primary protons, McDonald and Webber [1959] estimated the flux of the sum of the splash and re-entrant proton albedo. The present results are consistent with these earlier measurements. Note however that the fluxes obtained by McDonald and Webber are the sum of the splash and return albedo, and should therefore be divided by a factor 2 for comparison with our data.

The flux of protons moving vertically downwards in the energy range from 37 MeV to 334 MeV was obtained in six intervals. In Table 1 we present the range in lead, the energy and the flux of the protons. Errors given here includes an estimate of the systematic experimental and statistical errors. The proton flux is corrected for interactions in lead and for dead time. The calculated flux of the secondary protons is given in Column 4, Table 1. We subtracted the contribution of the secondary protons and extrapolated the spectrum to the top of the atmosphere by considering ionization losses only. The resulting spectrum is shown in the

last two columns of the table. We also plotted the return albedo spectrum in Figure 6 for comparison with the splash proton energy spectrum. The two spectra agree within experimental errors. E. C. Ray [1962] has calculated the vertical flux of the re-entrant proton albedo at 85 MeV for Sioux Falls, S. D. He obtained a flux of 1.17 protons/(m^2 sec ster MeV), which was considered to be high. We were able to point out an error in his calculation which we corrected. After this correction, the flux was reduced to 0.43 protons/(m^2 sec ster MeV) at 85 MeV. Ray recently repeated his calculations (private communication 1965), including the effects of nuclear interactions of protons and α-particles in air and of the trajectories. This improved value of the proton flux is 0.41 protons/(m^2 sec ster MeV) under the same conditions as before. This flux is in good agreement with our measurement at Palestine, Texas, and his calculated value has been included in Figure 6.

(B) Electron Albedo

(1) Splash Albedo Electron Flux vs. Depth

The splash albedo electrons behave similar to the splash albedo protons. Their flux as a function of depth is shown in Figure 7 for two energy intervals, 10 to 100 MeV and 100 to 1100 MeV. Again the difference between the flux observed at floating altitude and the flux extrapolated to the top of the atmosphere is negligible. Hence, also the electron splash albedo spectra observed at 3.8 g/cm^2 were considered to be identical with the spectra at the top of the atmosphere.

(2) Comparison of Splash and Re-entrant Electron Albedo Energy Spectra

In this section we shall discuss the electron albedo spectra. As explained earlier, in the case of protons, also the splash electron spectrum at 3.8 g/cm^2 atmospheric depth is closely the same as at the top of the atmosphere. In

columns 1 and 2 of Table II we present the energy and the flux of the splash electrons including the sum of systematic experimental and statistical errors. Stopping muons in the lead absorber having range between 40 and 115 g/cm^2 and therefore an energy between 60 MeV and 160 MeV cannot be distinguished from stopping electron showers. These muons have sufficient energy to give Cerenkov light in the lucite C_1 counter and appear like electrons. A calculation has been made to estimate the flux of μ -mesons in this energy interval (See Appendix). The result of this calculation is shown in Column 3 and 4, Table II. In column 5 we present the splash albedo electron spectrum which includes a correction for muons.

Turning to the re-entrant electrons, one finds that in the case of vertically downward moving electrons, the largest background is due to secondary electrons. This was discussed in deatil in section V(B). The measured flux of electrons moving downwards in the 10 to 1100 MeV energy range at a depth of 4 g/cm^2 at Palestine, Texas is shown in Figure 8. The contribution of the secondary electrons at 4 g/cm^2, which was calculated by Verma [1966], is also plotted in Figure 8 and the error limits of the calculation are shown. Taking the difference between the measured flux and the secondaries, we obtained the energy spectrum of the re-entrant albedo electrons at floating altitude (depth 4 g/cm^2). Extrapolation of this spectrum to the top of the atmosphere was carried out, including energy losses due to ionization and Bremsstrahlung, and the result is shown in Figure 9. For comparison, we also plotted in the same figure the splash albedo electron spectrum observed at 3.8 g/cm^2. We do not consider the difference between the two spectra significant. Each was approximated by a power law, using the least squares method, with the result:

$$\left(\frac{dJ}{dE}\right)_{Sp.El.} = (5.4 \pm 0.5)\ 10^2\ E^{-(1.29 \pm .06)}\ (m^2\ sec\ ster\ MeV)^{-1};\quad 10 \leq E \leq 1100\ MeV$$

$$\left(\frac{dJ}{dE}\right)_{Re.\ El.} = (5.9 \pm 0.9)\ 10^2\ E^{-(1.44 \pm .09)}\ (m^2\ sec\ ster\ MeV)^{-1};\quad 20 \leq E \leq 1250\ MeV$$

In Figure 10 we have summarized all measurements of the re-entrant electron albedo flux and energy spectrum without correcting for atmospheric secondary electrons. Schmoker and Earl [1965] have measured the flux of re-entrant electrons in the 45 MeV to 150 MeV and 1 BeV to 4.5 BeV energy intervals at depths of 6 and 4.5 g/cm^2 at San Angelo, Texas and Minneapolis, Minnesota in 1962 and 1963 respectively. Bleeker et al. [1965] have measured the energy spectrum in the energy interval from 0.4 BeV to 1.4 BeV at a depth of 10 g/cm^2 over DeBilt, Netherlands in summer 1965. Daniel and Stephens [1965] measured the spectrum at 10 g/cm^2 at Hyderabad, India in April, 1963. In their experiment the sample of particles is very small and therefore of limited statistical accuracy. The flux of re-entrant albedo electrons between 2 to 6 BeV based upon the work by Daniel and Stephens is also included in Figure 10.

VII. Summary

We have investigated the differential energy spectra and the fluxes of the splash and re-entrant albedo protons in the energy range from 37 to 334 MeV at Palestine, Texas. We have shown that the flux and the energy spectrum of the splash albedo protons agree with the energy spectrum of the re-entrant albedo protons, as has been expected on the basis of motion of the secondary particles in the geomagnetic field. If we compare the spectrum of the re-entrant protons in the 76 to 350 MeV region at the top of the atmosphere with the primary proton energy spectrum in the same energy region and at the same time as observed at Churchill [V. B. Balasubrahmanyan

et al. 1965], one finds that the two spectra are very different and have different slopes. The flux of the re-entrant protons is about 15% of the primary proton flux in the 90 - 200 MeV energy range, and about 6% in the 200 - 350 MeV energy region.

In the same experiment, we have also investigated the differential energy spectra and the fluxes of the splash and re-entrant albedo electrons in the 10 to 1100 MeV energy region. In this case the spectra and the fluxes are also similar to each other as expected. If one compares the flux and the spectrum of the re-entrant electron albedo in the energy region from 10 MeV to 500 MeV with those of the primary electrons in the same energy region observed at Churchill at about the same time [L'Heureux 1966] , one finds that the flux and the energy spectrum are very similar. The similarity of the shape of the spectra may be explained by assuming that in both the cases, the electrons are produced by the same process, namely nuclear interactions between protons and the nuclei in the atmosphere in one case and with the galactic matter in the other case. The fact that the magnitude of the fluxes are also similar must be considered fortuitous.

Acknowledgements

The author wishes to thank his faculty sponsor, Professor Peter Meyer, for suggesting this problem and for many helpful discussions and continued support during the time this work was carried out.

Many thanks are due to H. Boersma and T. Burdick for invaluable help in the electronics work and to R. Ekstrom, Asha L. Verma and Lee Hecht for their help in the data analysis. We are greatly indebted to A. Hoteko and W. Johnson for the

mechanical construction work of the project. We are indebted to the NCAR Balloon Facility and Raven Industries for the successful balloon launchings and very prompt recovery of the scientific payloads.

Appendix

Here we briefly outline the method used to estimate the contribution of muons of energy between 60 and 160 MeV in the observed energy spectrum of the splash albedo electrons. We assume that in the energy region of interest (300 MeV to 1100 MeV for electrons; 60 MeV to 160 MeV for muons) the energy spectrum of the splash albedo electrons and muons can be represented as

$$N(E_e) = K_e \; E^{-\gamma_e} \tag{1}$$

$$N(E_\mu) = K_\mu \; E^{-\gamma_\mu} \tag{2}$$

Using a method developed earlier to evaluate the spectrum of secondary particles [Verma 1966], we find

$$\gamma_\mu = \gamma_e - 1 \tag{3}$$

Assume that N_1 is the sum of the number of electrons having an energy between E_e^1 and E_e^2 and of muons having an energy between E_μ^1 and E_μ^2

then

$$N_1 = \int_{E_e^1}^{E_e^2} K_e \, E_e^{-\gamma_e} \, dE_e + \int_{E_\mu^1}^{E_\mu^2} K_\mu \, E_\mu^{-(\gamma_e - 1)} \, dE_\mu \tag{4}$$

$$N_1 = a_{11} K_e + a_{12} K_\mu \tag{5}$$

where

$$a_{11} = \int_{E_e'}^{E_e^2} E_e^{-\gamma_e} dE_e \quad ; \quad a_{12} = \int_{E_\mu'}^{E_\mu^2} E_\mu^{-(\gamma_e - 1)} dE_\mu \tag{6}$$

Similarly, if N_2 is the sum of the number of electrons having energy between E_e^2 and E_e^3 and of muons having an energy between E_μ^2 and E_μ^3 then

$$N_2 = a_{21} K_e + a_{22} K_\mu \tag{7}$$

where a_{21} and a_{22} are constants similar to those of Eq.(6). All the constants a_{11}, a_{12}, a_{21} and a_{22} are evaluated using the γ_e of the observed splash albedo electron energy spectrum without muon correction. N_1 and N_2 are observed quantities. Solving the simultaneous Eqs. (5) and (6) we obtained the value of K_e and K_μ. Knowing the values of the constants a_{12}, a_{22} and K_μ we estimated the contribution of muons in two energy intervals. Using the values of K_e and K_μ we also estimated the flux of splash albedo electrons and muons in third energy interval which agrees with the observed value. The estimated contribution of muons in three energy intervals is given in Columns 3 and 4, Table II.

REFERENCES

Balasubrahmanyan, V. K., D. E. Hagge, G. H. Ludwig and F. B. McDonald, Galactic cosmic rays at solar minimum, Proc. Int. Conf. Cosmic Rays, London, 1, 427-436, 1965.

Bleeker, J. A. M., J. J. Burger, A. Scheepmaker, B. N. Swanenburg and Y. Tanaka, A balloon observation of high energy electrons, The Int. Conf. on Cosmic Rays, London, 1, 327-330, 1965.

Daniel, R. R. and S. A. Stephens, Electron component of the primary cosmic radiation at energies $\gtrsim$ 15 GeV, Phys. Rev. Letters, 15, 769-772, 1965.

Hasegawa, H., S. Nakagawa, and E. Tamai, Measurement of hydrogen nuclei in primary cosmic rays, Nuovo Cimento, 36, 18-34, 1965.

L'Heureux, J., The primary cosmic ray electron spectrum near solar minimum (to be published, 1966).

Lord, J. J., The altitude and latitude variation in the rate of occurrence of nuclear disintegrations produced in the stratosphere by cosmic rays, Phys. Rev. 81, 901-909, 1951.

McDonald, F. B., Primary cosmic-ray proton and alpha flux near the geomagnetic equator, Phys. Rev. 109, 1367-1375, 1958.

McDonald, F. B. and W. R. Webber, Proton component of the primary cosmic radiation, Phys. Rev. 115, 194-205, 1959.

Meyer, P. and R. Vogt, Primary cosmic ray and solar protons. II, Phys. Rev. 126, 2275-2279, 1963.

Ormes, J and W. R. Webber, Measurements of low-energy protons and alpha particles in the cosmic radiation, Phys. Rev. Letters 13, 106-108, 1964.

Ray, E. C., Re-entrant cosmic ray albedo, J. Geophys. Res. 67, 3289-3291, 1962.

Rich, M. and R. Madey, Range energy tables, UCRL- (2301), March 1954.

Schmoker, J. W. and J. A. Earl, Magnetic cloud chamber observations of low energy cosmic ray electrons, Phys. Rev. 138, B300-302 , 1965.

Treiman, S. B., The cosmic-ray albedo, Phys. Rev. 91, 957-959, 1953.

Verma, S. D., A calculation of the flux and energy spectrum of secondary electrons at high altitudes in the atmosphere, Enrico Fermi Inst. Notes No. 66-44, 1966.

Vogt, R., Primary cosmic ray and solar protons, Phys. Rev. 125, 366-377, 1962, and Ph.D. thesis submitted to the University of Chicago.

TABLE I

The flux of re-entrant albedo protons under 4 g/cm^2 atmospheric depth and extrapolated to the top of the atmosphere

Atmospheric Depth 4 g/cm^2				Extrapolated to the top of the Atmosphere	
Range Interval in Pb (g/cm^2)	Energy Interval (MeV)	Observed Flux $(m^2 sec.ster.)^{-1}$	Secondary Flux $(m^2 sec.ster.)^{-1}$	Energy Interval (MeV)	Re-entrant Flux $(m^2 sec.ster.)^{-1}$
$1.95 \leq R < 4.1$	$37 \leq E < 52$	10.5 ± 2.3	5.4 ± 1.1	$76 \leq E < 88$	6.0 ± 2.6
$4.1 \leq R < 23.5$	$52 \leq E < 124$	17.9 ± 4.4	9.2 ± 1.9	$88 \leq E < 147$	9.5 ± 4.8
$23.5 \leq R < 41.0$	$124 \leq E < 174$	7.3 ± 1.3	2.5 ± 0.5	$147 \leq E < 193$	4.8 ± 1.4
$41.0 \leq R < 62.5$	$174 \leq E < 225$	5.3 ± 1.1	1.53 ± 0.3	$193 \leq E < 241$	3.72 ± 1.1
$62.5 \leq R < 88.0$	$225 \leq E < 275$	4.8 ± 1.1	1.15 ± 0.3	$241 \leq E < 290$	3.67 ± 1.1
$88.0 \leq R < 118.0$	$275 \leq E < 334$	3.7 ± 0.9	0.9 ± 0.2	$290 \leq E < 349$	2.8 ± 0.9

Table II

The Flux of Splash Albedo Electrons at 3.8 g/cm^2 Atmospheric Depth

Energy Interval (MeV)	Observed Flux $(m^2 sec.ster.)^{-1}$	Muon Contribution		Corrected Splash Albedo Electron Flux $(m^2 sec.ster.)^{-1}$
		Muon Energy (MeV)	Flux $(m^2 sec.ster.)^{-1}$	
10 - 100	467 ± 48	-----	-----	467 ± 48
100 - 300	134 ± 15	-----	-----	134 ± 15
300 - 500	51.2 ± 5	63 - 90	5.4 ± 1.8	45.8 ± 5.4
500 - 700	34 ± 4	90 - 122	6.3 ± 2.0	27.7 ± 4.6
700 - 1100	43 ± 7	122 - 170	8.6 ± 1.6	34.4 ± 8.0

Figure Captions

Figure 1. Schematic cross-section of the detector system.

Figure 2. Flux vs. atmospheric depth for vertically downward moving protons in the energy interval from 37 MeV to 334 MeV at Palestine, Texas. _____ ..... calculated secondary proton flux; _____ . _____ . _____ Calculated incident vertical flux (matched with experimental value at 4 g/cm^2); ---- sum of the calculated secondary flux and the incident flux (re-entrant proton albedo).

Figure 3. Flux vs. atmospheric depth for vertically downward moving electrons in the energy interval from 10 MeV to 100 MeV and from 100 MeV to 1100 MeV at Palestine, Texas. _____ ..... calculated secondary electron flux; _____ . _____ . calculated incident vertical flux (matched with experimental value at 4 g/cm^2); ---- sum of the calculated secondary flux and the incident flux (re-entrant electron albedo).

Figure 4. Flux vs. atmospheric depth for vertically upward moving protons in the energy interval from 37 to 334 MeV at Palestine, Texas.

Figure 5. Splash albedo proton energy spectrum observed at 3.8 g/cm^2 at Palestine, Texas and measurements of other workers.

Figure 6. Re-entrant and splash albedo proton energy spectra extrapolated to 0 g/cm^2 at Palestine, Texas. □ Re-entrant proton flux calculated by Ray [1962] for Sioux Falls, South Dakota.

Figure 7. Flux vs. atmospheric depth for vertically upward moving electrons in the energy interval from 10 MeV to 100 MeV and from 100 MeV to

1100 MeV at Palestine, Texas.

Figure 8. Re-entrant albedo electron energy spectrum at 4.0 g/cm^2 at Palestine, Texas. Solid line: energy spectrum of secondary electrons calculated by Verma [1966]; dashed lines: error limits of the calculations.

Figure 9. Splash and re-entrant albedo electron flux and energy spectrum extrapolated to the top of the atmosphere at Palestine, Texas.

Figure 10. Summary of all measurements of the re-entrant albedo electron energy spectrum.

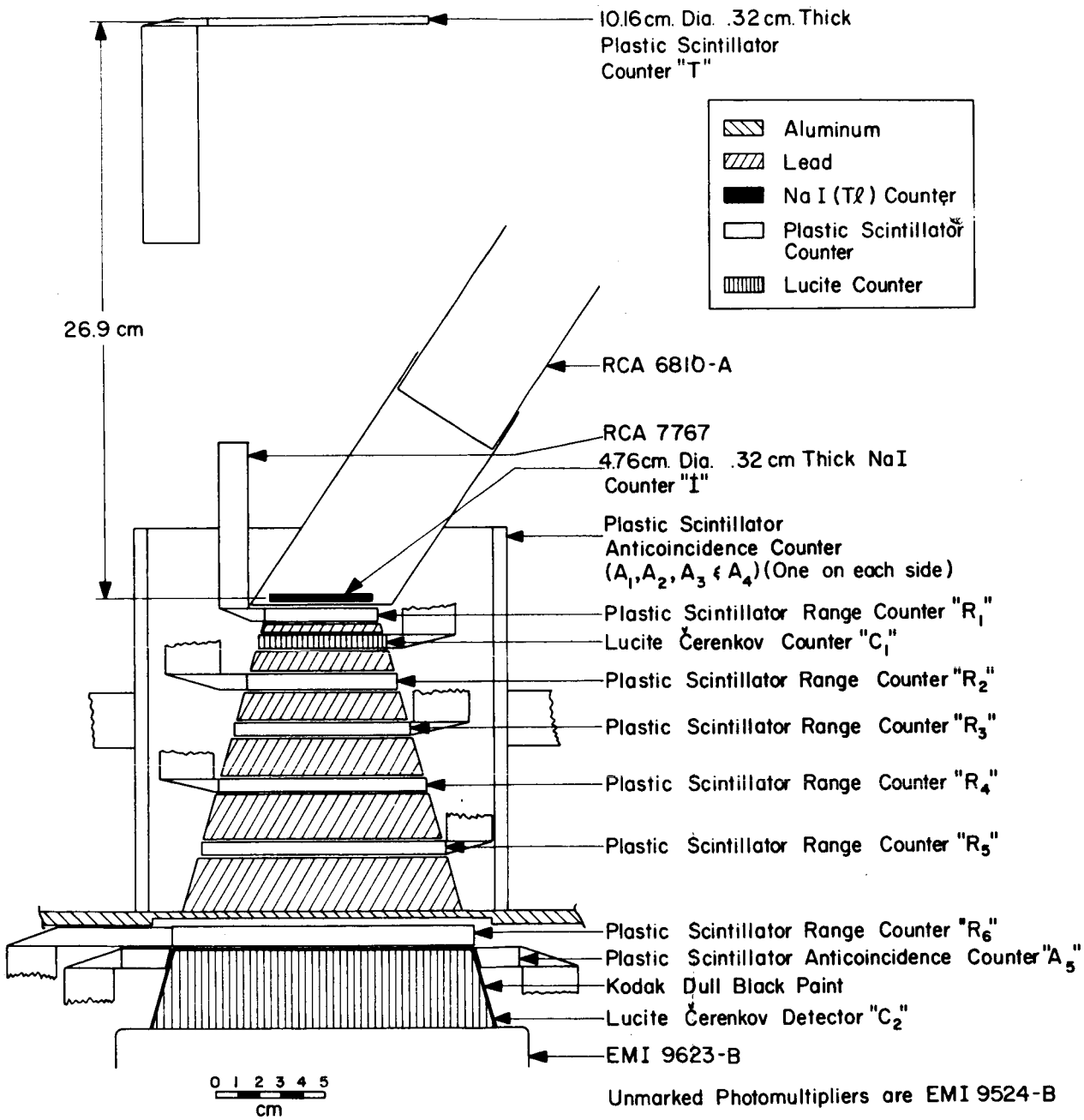
10.16cm. Dia. .32 cm. Thick
Plastic Scintillator
Counter "T"
Aluminum
Lead
Na I (Tℓ) Counter
Plastic Scintillator Counter
Lucite Counter
26.9 cm
RCA 6810-A
RCA 7767
4.76cm. Dia. .32 cm Thick NaI
Counter "I"
Plastic Scintillator
Anticoincidence Counter
(A_1, A_2, A_3 & A_4) (One on each side)
Plastic Scintillator Range Counter "R_1"
Lucite Čerenkov Counter "C_1"
Plastic Scintillator Range Counter "R_2"
Plastic Scintillator Range Counter "R_3"
Plastic Scintillator Range Counter "R_4"
Plastic Scintillator Range Counter "R_5"
Plastic Scintillator Range Counter "R_6"
Plastic Scintillator Anticoincidence Counter "A_5"
Kodak Dull Black Paint
Lucite Čerenkov Detector "C_2"
EMI 9623-B
0 1 2 3 4 5
cm
Unmarked Photomultipliers are EMI 9524-B

Figure 1

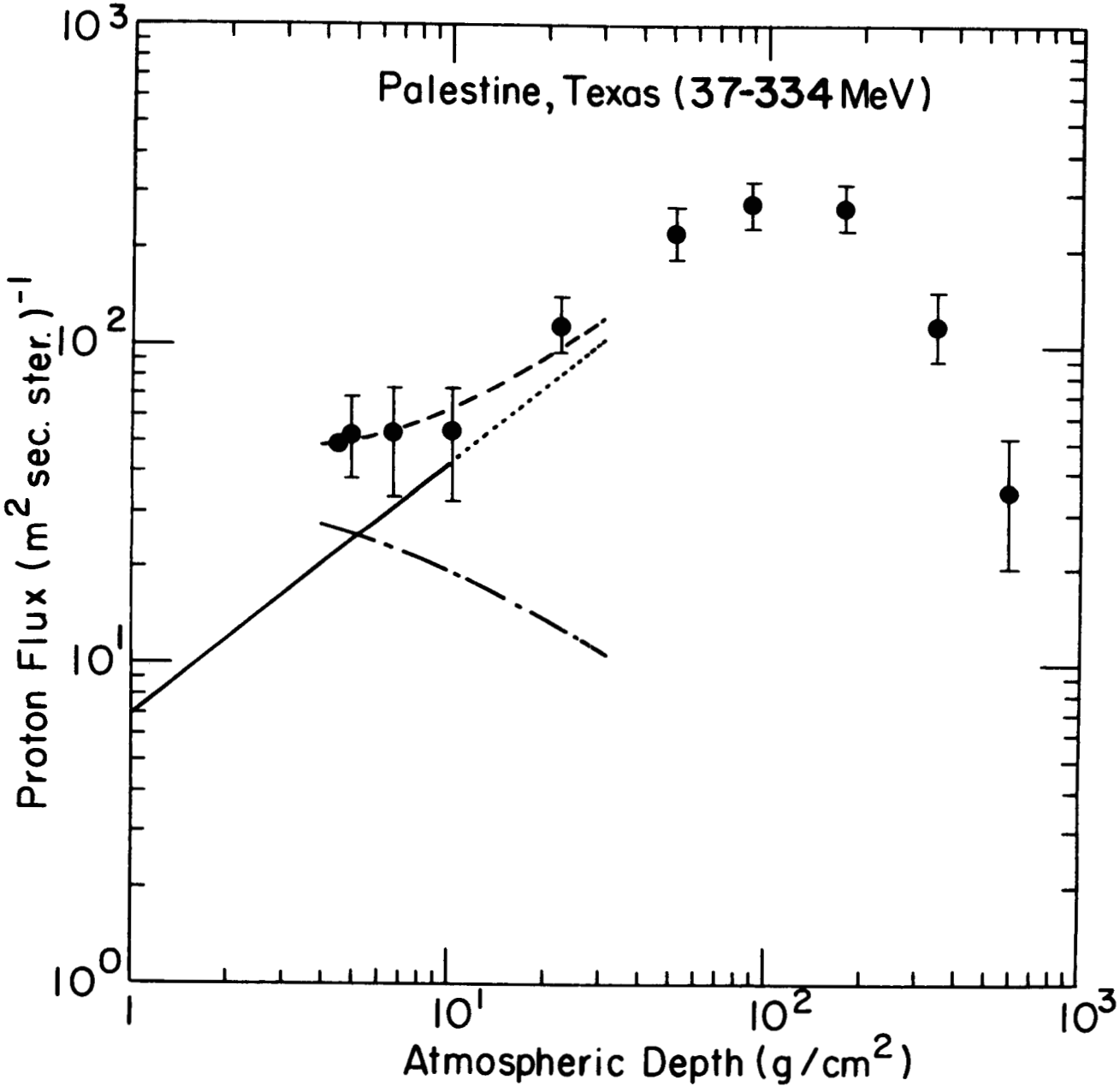
Palestine, Texas (37-334 MeV)
Proton Flux (m^2 sec. ster.)$^{-1}$
Atmospheric Depth (g/cm^2)
10^3
10^2
10^1
10^0
1
10^1
10^2
10^3

Figure 2

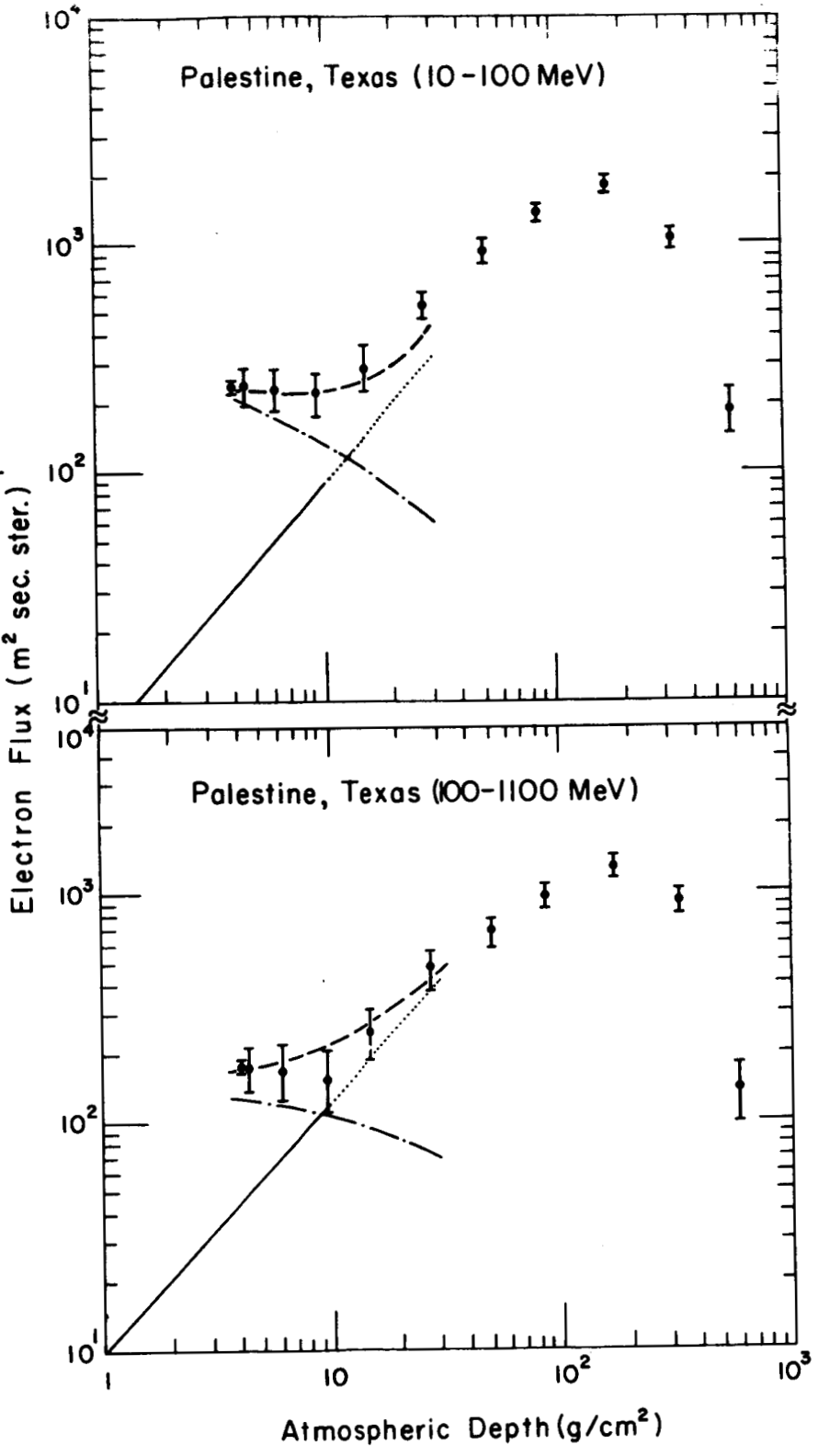
Palestine, Texas (10-100 MeV)
Palestine, Texas (100-1100 MeV)
Electron Flux (m² sec. ster.)⁻¹
Atmospheric Depth (g/cm²)
10⁴
10³
10²
10¹
1
10
10²
10³

Figure 3

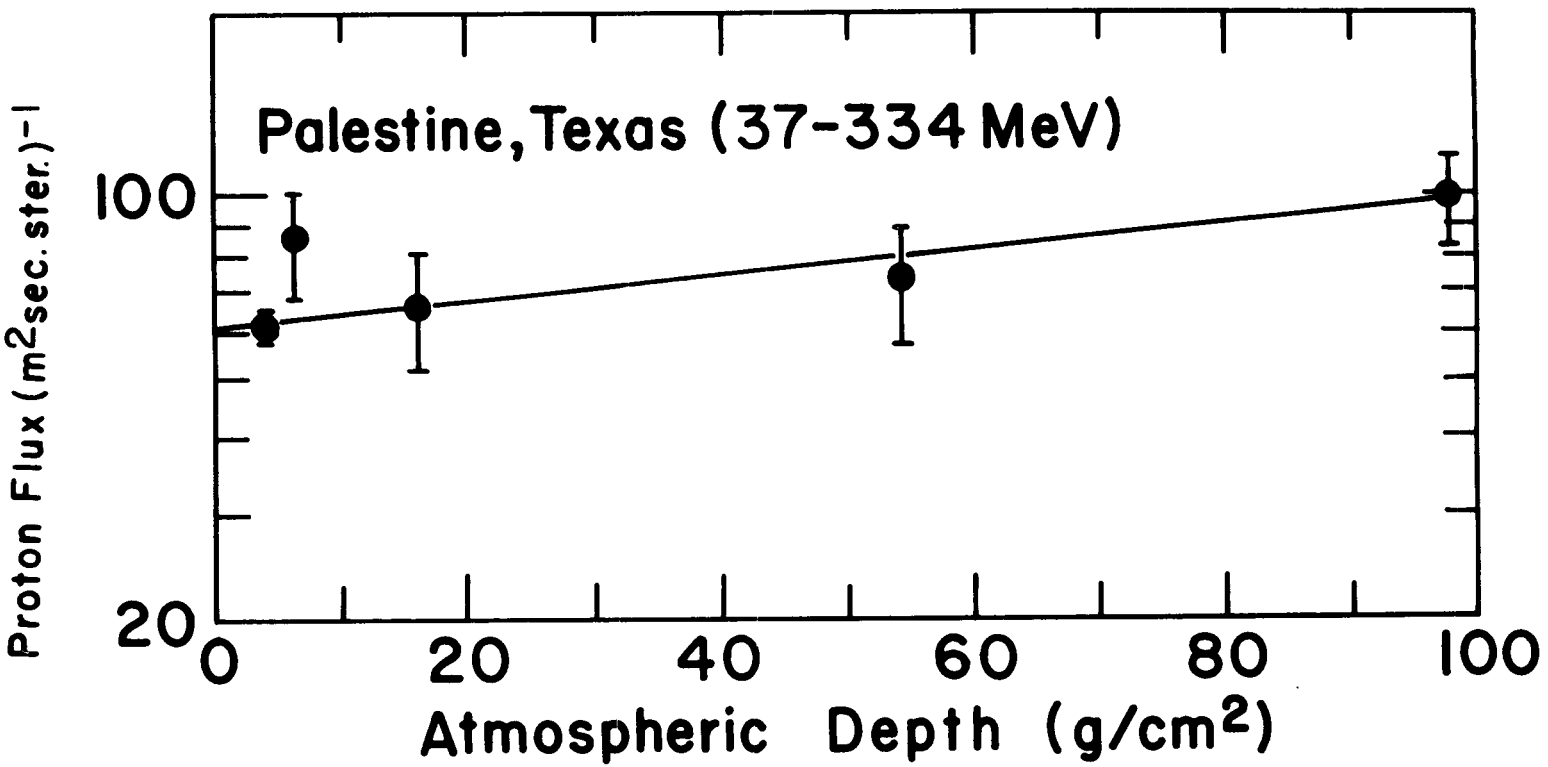
Palestine, Texas (37-334 MeV)
Proton Flux (m²sec.ster.)⁻¹
100
20
0
20
40
60
80
100
Atmospheric Depth (g/cm²)

Figure 4

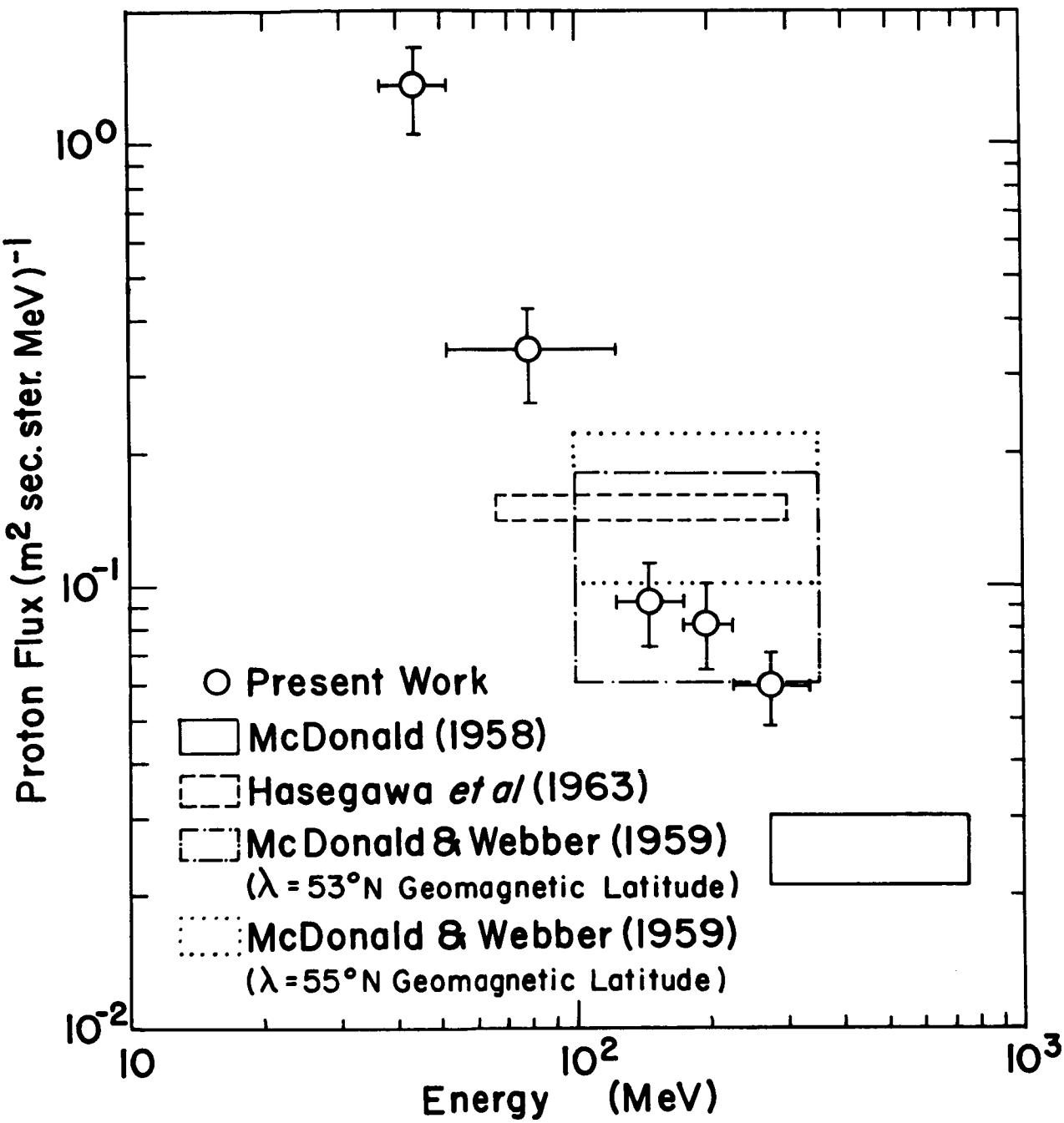
Proton Flux (m² sec. ster. MeV)⁻¹
10⁰
10⁻¹
10⁻²
10
10²
10³
Energy (MeV)
O Present Work
McDonald (1958)
Hasegawa et al (1963)
McDonald & Webber (1959)
(λ = 53°N Geomagnetic Latitude)
McDonald & Webber (1959)
(λ = 55°N Geomagnetic Latitude)

Figure 5

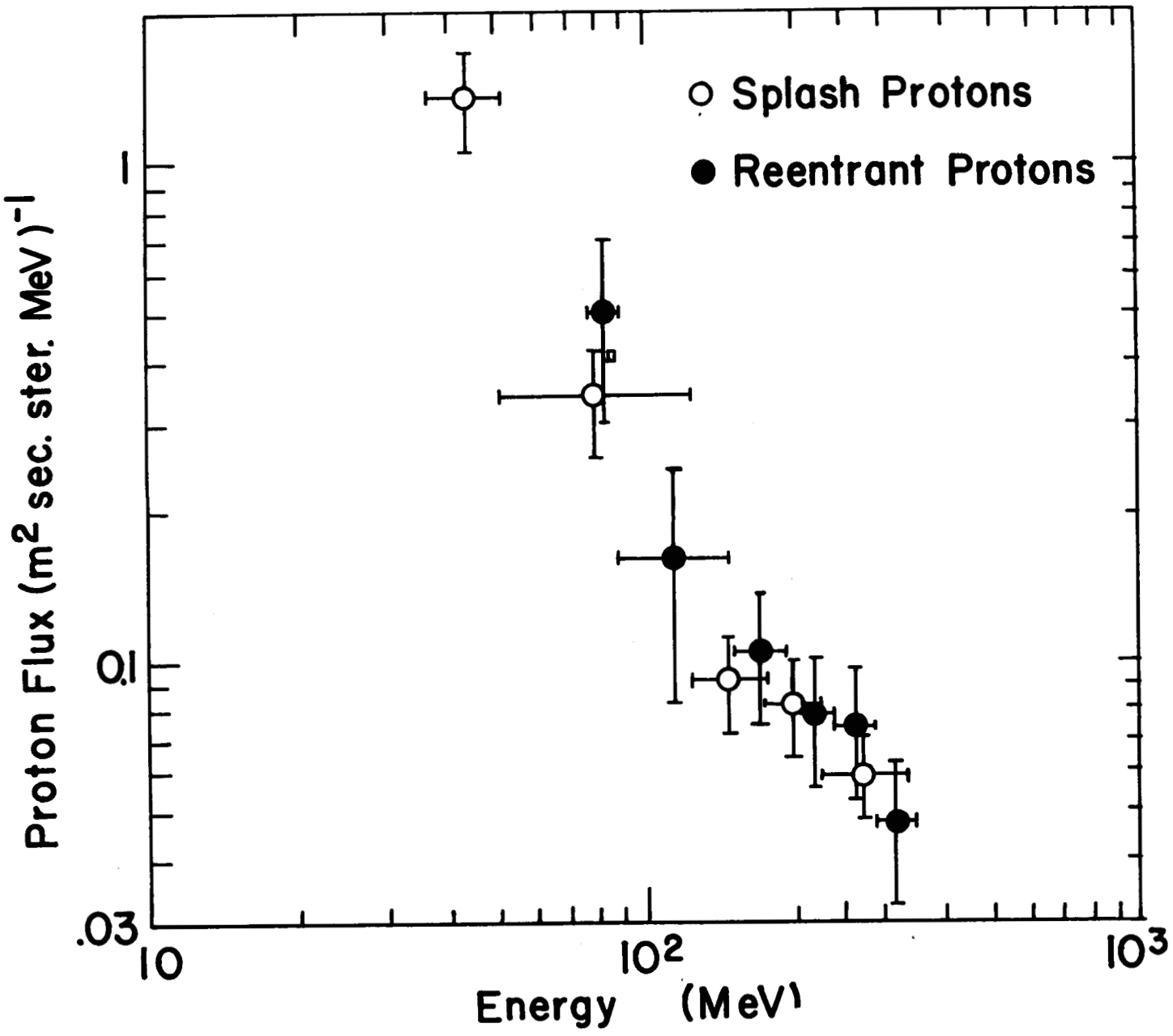
Splash Protons
Reentrant Protons
Proton Flux (m² sec. ster. MeV)⁻¹
1
0.1
.03
10
10²
10³
Energy (MeV)

Figure 6

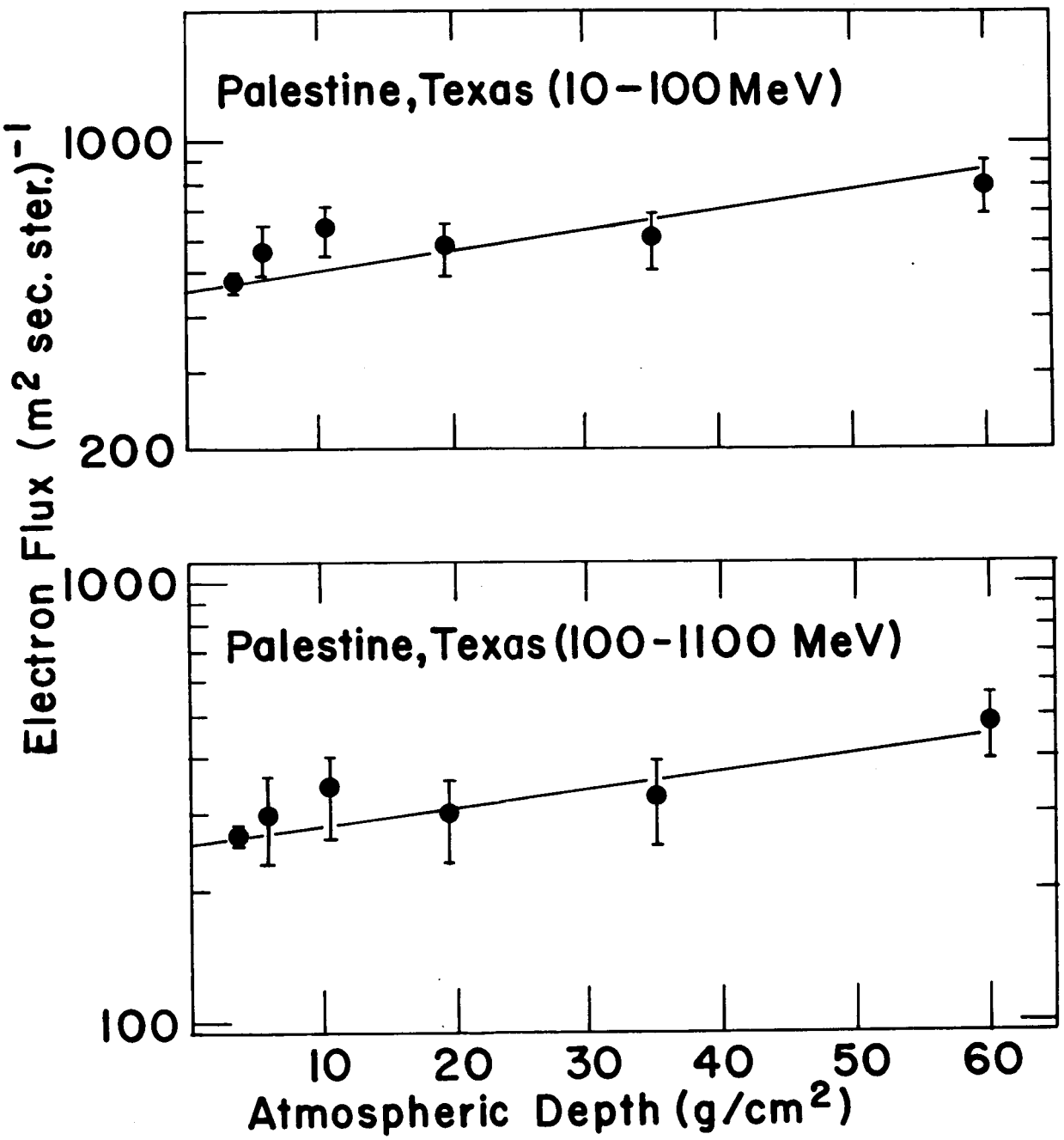
Palestine, Texas (10–100 MeV)
1000
200
Palestine, Texas (100–1100 MeV)
1000
100
Electron Flux (m² sec. ster.)⁻¹
10
20
30
40
50
60
Atmospheric Depth (g/cm²)

Figure 7

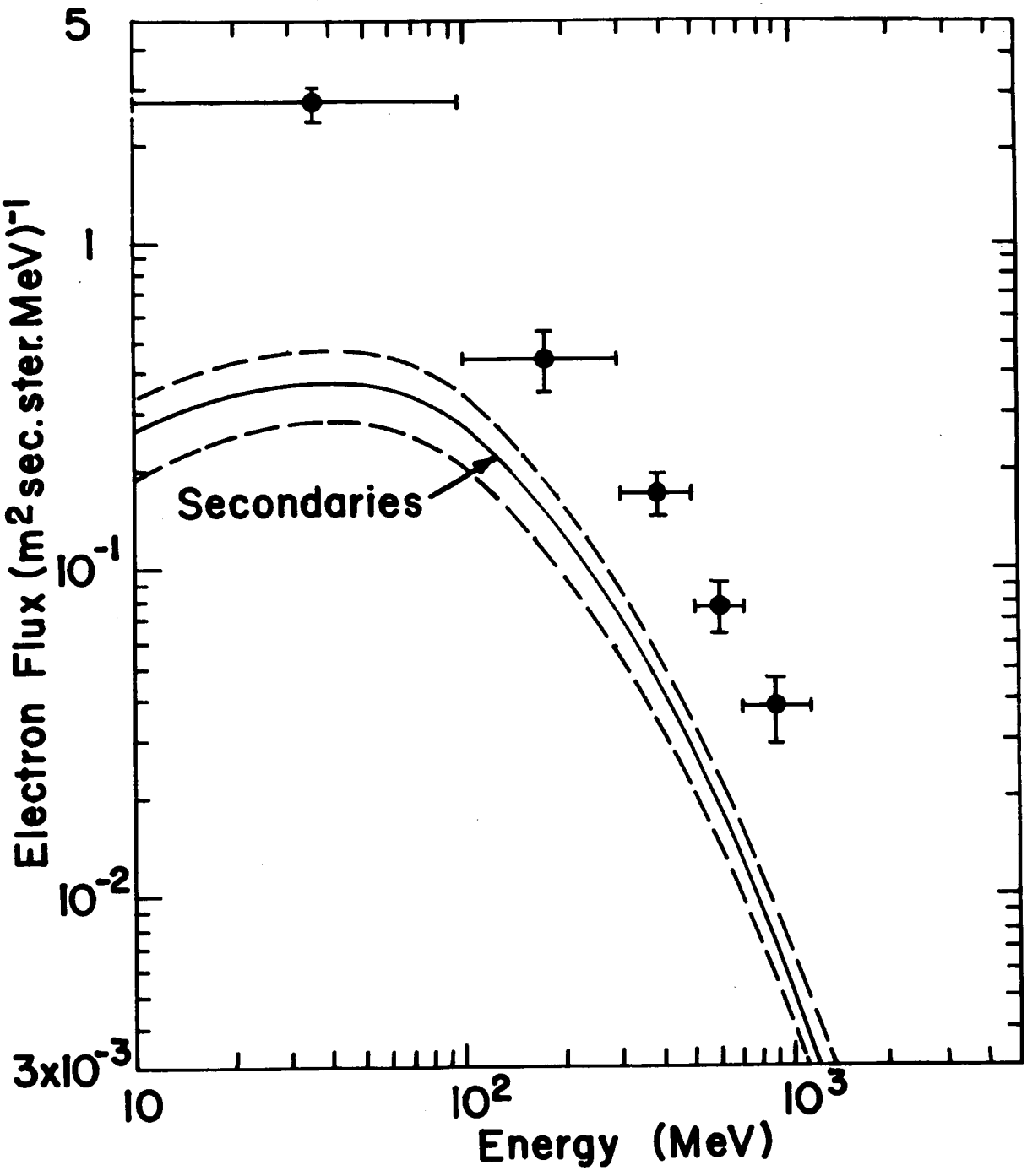
5
1
10^{-1}
10^{-2}
$3x10^{-3}$
Electron Flux (m^2 sec. ster. MeV)$^{-1}$
Secondaries
10
10^2
10^3
Energy (MeV)

Figure 8

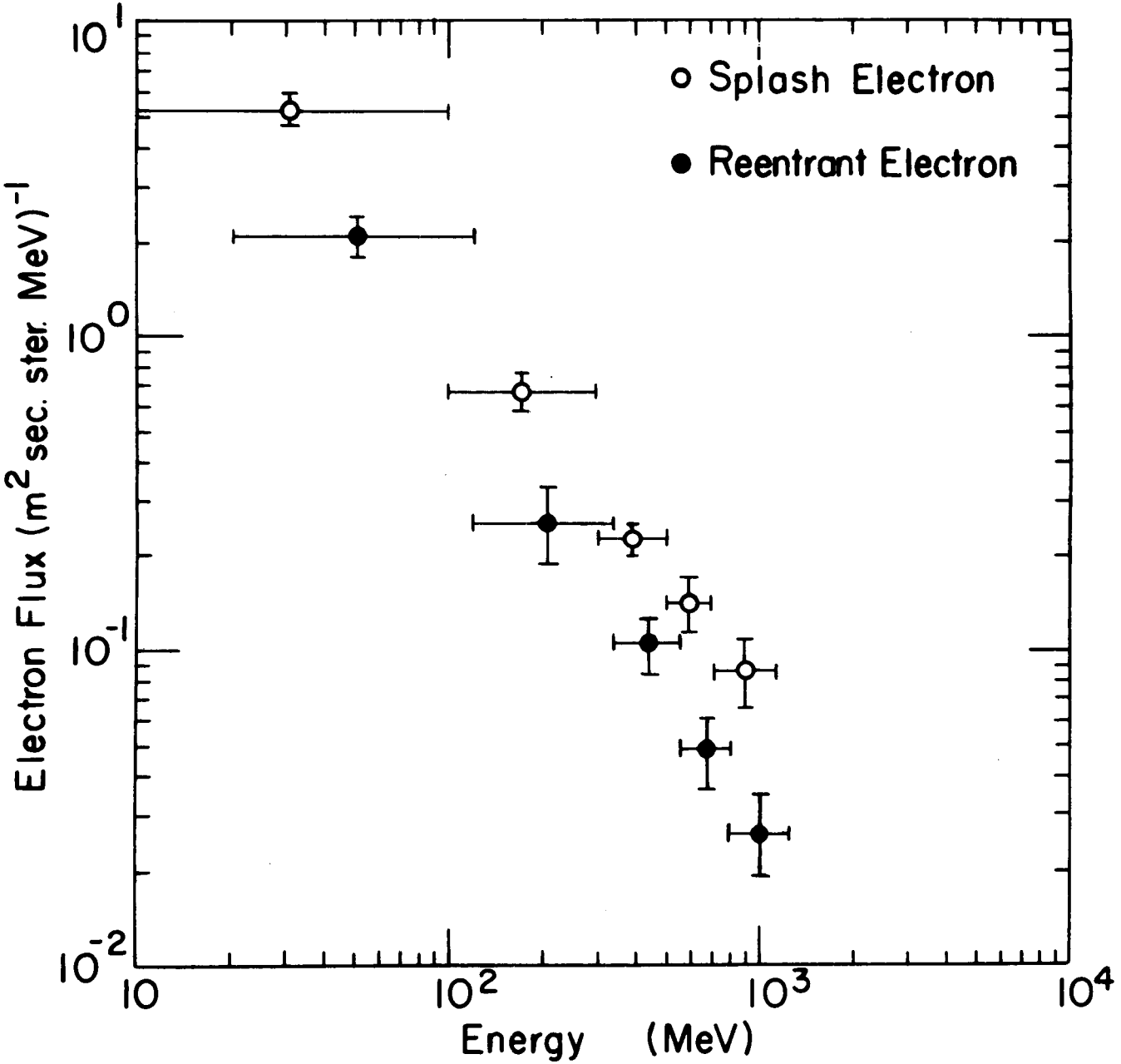
Splash Electron
Reentrant Electron
Electron Flux (m^2 sec. ster. MeV)$^{-1}$
10^1
10^0
10^{-1}
10^{-2}
10
10^2
10^3
10^4
Energy (MeV)

Figure 9

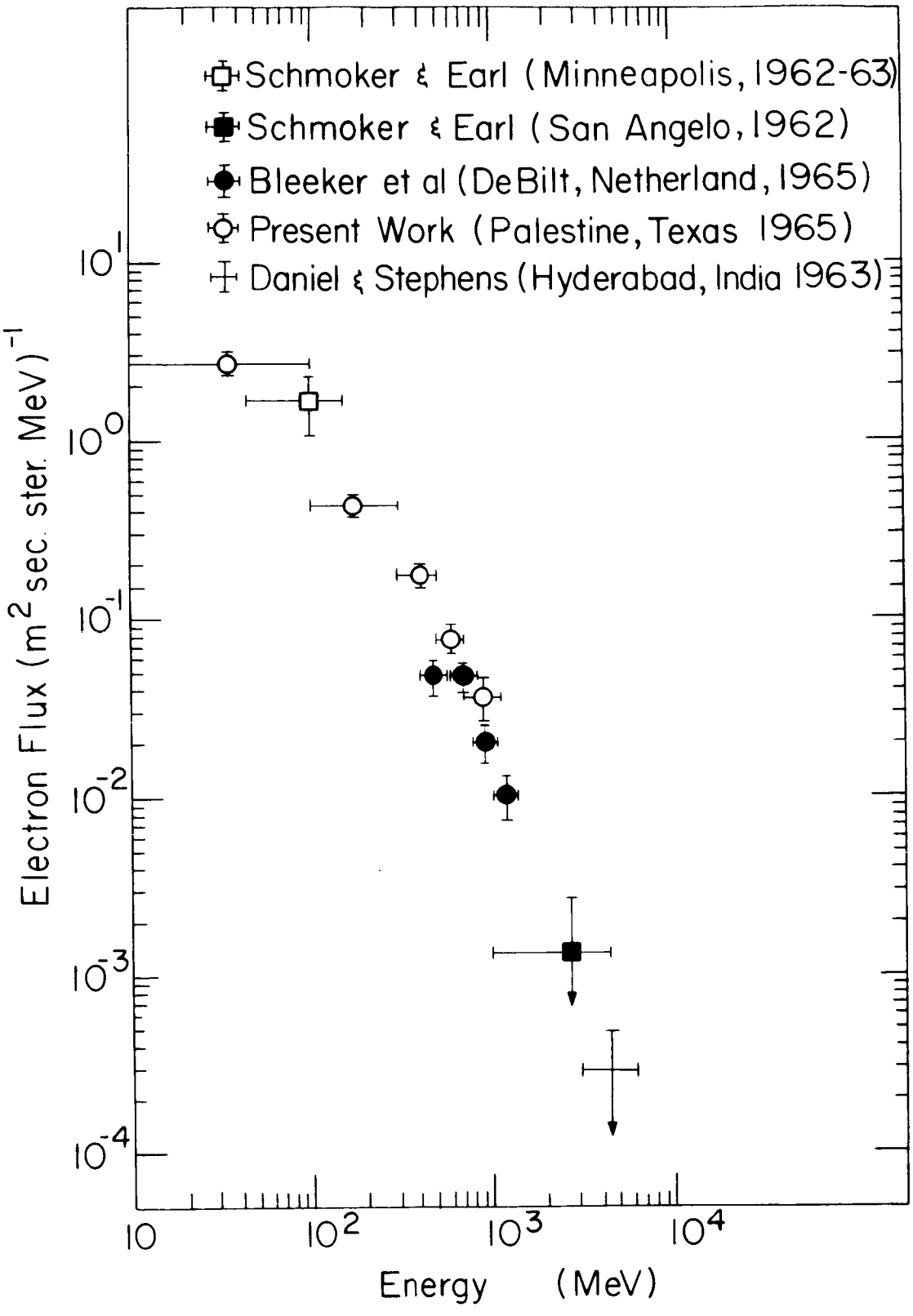
Schmoker & Earl (Minneapolis, 1962-63)
Schmoker & Earl (San Angelo, 1962)
Bleeker et al (DeBilt, Netherland, 1965)
Present Work (Palestine, Texas 1965)
Daniel & Stephens (Hyderabad, India 1963)
Electron Flux (m² sec. ster. MeV)⁻¹
10¹
10⁰
10⁻¹
10⁻²
10⁻³
10⁻⁴
10
10²
10³
10⁴
Energy (MeV)

Figure 10